

In-plane light-hole g factor in strained cubic heterostructures

A. A. Kiselev* and K. W. Kim

Department of Electrical and Computer Engineering, North Carolina State University, Raleigh, North Carolina 27695-7911

E. Yablonovitch

Department of Electrical Engineering, University of California, Los Angeles, Los Angeles, California 90024

(Received 7 March 2001; published 5 September 2001)

In the context of a proposed design of a solid-state receiver for quantum communications, we consider the Zeeman splitting of the light-hole states in strained cubic heterostructures with an in-plane external magnetic field. The choice of interband optical transitions that allows coherent transfer of photon polarization to electron spin suggests that the magnitude of corresponding g factor component will be a critically important quantity for the success of such devices. Our approach allows a straightforward calculation of this parameter and incorporates the quantum confinement, heterolayers composition, and strain effects on the g factor.

DOI: 10.1103/PhysRevB.64.125303

PACS number(s): 73.21.-b, 71.18.+y, 71.20.-b

I. INTRODUCTION

Secure quantum communication schemes are based on the entanglement of coherent quantum states (see Ref. 1 and references therein). To achieve this for practical use, one must be able to transmit quantum information over long distances, perform elements of quantum computing to execute error correction, and retain the information without decoherence. Such rigorous conditions require the development of a system that is capable of receiving quantum information in the form of coherent photon states, storing the information, performing the necessary operations, and then retransmitting the photon signal while maintaining quantum coherence throughout the process. In particular, it was proposed to transfer quantum information from photons to atoms trapped in high- Q optical cavities.^{2,3} It is also well known that information in the form of photon polarization can be transferred to electron spin in semiconductors and vice versa in absorption and emission processes.⁴ Hence, utilizing the electron spin degree of freedom in solids provides a clear pathway to the development of a practical quantum communication system. Such a system could reliably function as a repeater to transmit quantum information over long distances and would accomplish a number of goals, including, for example, secure data transmission.

A promising scheme, based on nanoscale semiconductor technology, was recently proposed to achieve this function.⁵ The suggested quantum communication system resembles conventional optical communication systems except that it takes advantage of particular photon absorption and emission selection rules. The design of the proposed receiver (and transmitter) needs to satisfy several demanding conditions simultaneously; one of them requires that both electron sublevels should couple optically to a single ground hole state, thus excluding entanglement with the quickly relaxing hole spin. Application of an external magnetic field leads to the desired valence-band splitting that should be sufficiently large to resolve hole sublevels spectroscopically. A proper experimental setup provides selection rules of the corresponding optical transitions that enable the transfer of photon polarization into the electron spin. This setup is thoroughly

discussed in Ref. 5; we follow those proposed selection rules and concentrate on the geometry with in-plane magnetic field.

The free-electron spin splitting factor, of value $g = 2.0023$, defines the influence of the external magnetic field on the doublet of otherwise degenerate electron states with spin $s = \pm 1/2$. Interaction of electron states with the lattice potential in crystals leads to the (often strong) renormalization of the g factor value.⁶ As one advances from bulk semiconductors to heterostructures, quantum confinement effects come into play that modify the g factor further. A comprehensive theory based on the $k\mathbf{p}$ method was developed to predict behavior of the electron g factor in low-dimensional systems including quantum wells, wires, and dots.^{7,8} Zeeman splitting for electrons was studied experimentally mainly in III-V and some II-VI quantum wells (QW's). A very close correspondence was found between theory and experiment, including overall dependence on the well layer width and more fine details such as electron g factor anisotropy.⁹ Some theoretical results were published for the longitudinal (magnetic field along the growth direction) heavy-hole (HH) g factor with moderate agreement with the so-far very scattered experimental data.^{10,11} There was a recent attempt to evaluate the transverse (in-plane) g factor for HH's and test the calculated value in the experiment.¹² Since the main contribution, caused by the interaction with the conduction band, is absent in this geometry, $|g_{\text{HH},\perp}|$ is very small (≈ 0.04). Thus, HH states cannot be sufficiently split by an in-plane magnetic field. They are not suitable for the quantum receiver, in which the hole states have to be resolved optically.

No work has been done for the light-hole (LH) states to the best of the author's knowledge. That is due, in part, to the fact that the much smaller effective mass and resulting higher quantization energies (compared to those for HH's) make it difficult even to detect LH states in typical heterostructures. Applied or lattice-mismatch-induced intrinsic strain can reverse this situation, making the LH the ground hole state in the structure with a QW. In this paper, we give a consistent theoretical analysis of the in-plane Zeeman effect for quantum-confined LH holes and evaluate possibilities to design structures with the desired property of a large g

factor for these valence states.

The rest of the paper is organized as follows. We start with a general description of the problem of calculating the Landé g factor for quantized electron (hole) states in heterostructures (Sec. II), discuss various $\mathbf{k}p$ models in order to identify the suitable one for our problem in Sec. III, and derive an equation for the in-plane LH g factor in the complete 8×8 $\mathbf{k}p$ model (Sec. IV), followed by numerical examples for both strained and unstrained QW's based on the InGaAsP heterosystems that are considered to be highly promising for optical applications (Sec. V). We conclude with a short summary.

II. GENERAL APPROACH

The general approach to calculate the g factor for a pair of Kramers-degenerate states in a heterostructure has already been described in the literature.^{7,8} The main result of the derivation is summarized as follows: Let us consider a multiband Hamiltonian $H(\mathbf{k})$ in the presence of an external magnetic field $\mathbf{B} = \nabla \times \mathbf{A}$. The procedure suggests two replacements $\mathbf{k} \rightarrow \mathbf{k} + \mathbf{A}/c$ (implicit magnetic field dependence, through a vector potential) and Hamiltonian $H \rightarrow H + \delta H_B$ (explicit term, describing a direct interaction with the magnetic field in the chosen model). Hereafter we use the atomic units $e = 1, \hbar = 1$, and $m_0 = 1$, where e is the electronic charge, \hbar is Planck's constant, and m_0 is the free-electron mass. As for the explicit magnetic field dependence of the effective Hamiltonian, if any is present, the terms iB_α/c can be treated merely as shortcuts for the anticommutators $k_{\alpha+1}k_{\alpha+2} - k_{\alpha+2}k_{\alpha+1}$ (cyclic permutation of indices $\alpha = x, y, z$ is used), thus converting the explicit perturbative term into its implicit, \mathbf{A} -dependent form. Alternatively, one could decide to evaluate these terms separately, resulting with the expansion

$$H\left(\mathbf{k} + \frac{1}{c}\mathbf{A}, B\right) \approx H(\mathbf{k}) + \frac{1}{c}\left\{ \mathbf{A} \frac{\partial H}{\partial \mathbf{k}} \right\} + \delta H_B. \quad (1)$$

Brackets $\{\}$ are used here as a reminder that the proper ordering of the operators should be preserved, with the vector potential \mathbf{A} taking the place of the wave vector \mathbf{k} as one derives the velocity operator $\partial H / \partial \mathbf{k}$ from the Hamiltonian H . We will return to the question of proper order of operators in the effective mass Hamiltonian later.

For a pair of states $|s\rangle$ ($s = \uparrow$ or \downarrow), the Zeeman contribution to the effective 2×2 Hamiltonian can be written as

$$\delta \mathcal{H}_{ss'} \equiv \frac{1}{4c} \sigma_{\alpha, ss'} g_{\alpha\beta} B_\beta = \frac{1}{c} \left\langle s \left| \mathbf{A} \frac{\partial H}{\partial \mathbf{k}} \right| s' \right\rangle + \langle s | \delta H_B | s' \rangle, \quad (2)$$

where $\hat{\sigma}_\alpha$ are the Pauli matrices and $1/4c$ stands for half of the Bohr magneton $\mu_B/2$ in atomic units. In general, an additional term should be included in the right-hand side of Eq. (2) to compensate the diamagnetic contribution to the effective Hamiltonian, but it is zero in symmetric structures when considering states at the subband extrema. Equation (2) can be considered as a definition of the g factor tensor with real components $g_{\alpha\beta}$.

Thus, in order to calculate the tensor $g_{\alpha\beta}$ it suffices to choose an adequate multiband $\mathbf{k}p$ model and find, first, the envelope functions φ_n in the multicomponent expansion $|s\rangle = \sum_n \varphi_n(\mathbf{r}) |n\rangle$ in the semiconductor structure at zero magnetic field and, second, evaluate the required matrix elements $\int d\mathbf{r} \varphi_n^*(\mathbf{r}) \{ \mathbf{A} \partial H / \partial \mathbf{k} \}_{nn'} \varphi_{n'}(\mathbf{r})$, $\int d\mathbf{r} \varphi_n^*(\mathbf{r}) \delta H_{B,nn'} \varphi_{n'}(\mathbf{r})$ where the integration is performed separately over all structure domains bounded by interfaces. The ability to evaluate directly these matrix elements depends on the proper choice of the vector potential gauge. For the quantized state in the QW with the growth direction z , the vector potential for the in-plane magnetic field should be taken in the form $A(z) = (B_y z, -B_x z, 0)$. We stress that here n is the index enumerating only the electronic bands in the constituent bulk semiconductors, not numerous individual quantum states.

III. CHOICE OF $\mathbf{k}p$ MODELS

It is well known that the electron spectrum in the crystal field potential of a semiconductor is found most conveniently within the (multiband) effective mass approximation. Luttinger was the first to consider the problem of calculating the dispersion of degenerate hole states (Γ_8 band) in GaAs-type semiconductors.^{13,14} The precision with which hole states can be obtained in the Luttinger model is determined by the ratio of the particle energy reckoned from the valence-band maximum to the relevant band gap. In wide-gap semiconductors, this smallest energy gap is the spin-orbit (SO) splitting between states in the Γ_8 and Γ_7 bands. While the Luttinger-Kohn 6×6 Hamiltonian describes the holes belonging to these bands in a consistent way,^{13,15} it takes into account the interaction of the Γ_8 and Γ_7 valence bands with the Γ_6 conduction band and the remote bands only to within terms quadratic in \mathbf{k} . At the same time, the consistent perturbative calculation of the dependence of the hole (or electron) g factor on the energy of a state in a heterostructure requires terms of the fourth order in the wave vector \mathbf{k} (see, e.g., Ref. 7), which is critical especially in narrow QW's with high quantization energies. Thus, a more elaborate approach should be applied. The simple Kane model¹⁶ takes fully and consistently into account the $\mathbf{k}p$ interaction of the Γ_6 , Γ_8 , and Γ_7 bands, but, for example, yields a wrong dispersion relation for the HH states, since the curvature of the HH band is governed primarily by the interaction with the higher conduction bands, $\Gamma_8^c + \Gamma_7^c$ (and all interactions with remote bands are neglected). Although it is not a matter of the highest concern while analyzing electron states in the conduction band, this leads to completely wrong results when focusing on the valence states.

Analyzing the merits and shortcomings of the various model Hamiltonians, we decided to use the complete 8×8 $\mathbf{k}p$ Hamiltonian^{17,18} in the hole g factor calculations, which takes the interaction of the Γ_6 , Γ_8 , and Γ_7 bands exactly into account (like the model of Kane) and does not omit the contributions of the remote bands by keeping them in a quadratic-in- \mathbf{k} approximation (similar to the Luttinger-Kohn approach). Figure 1, graphically presenting the involved band structure parameters and $\mathbf{k}p$ interactions for a typical III-V semiconductor, uses the following notation: E_g is the

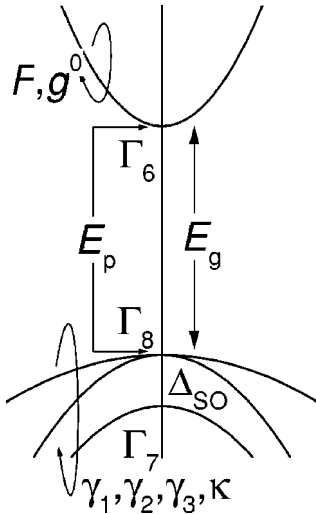


FIG. 1. Band diagram of a typical III-V semiconductor.

band gap, Δ is the spin-orbit splitting of the Γ_8 and Γ_7 bands, the E_p parameter characterizes the $\mathbf{k}p$ interaction of the valence- and conduction-band states and is related to the interband matrix element of the angular momentum operator through $E_p = 2P^2$, and the parameter F determines the conduction band curvature due to the interaction with the remote bands. The modified Luttinger parameters $\gamma_1, \gamma_2, \gamma_3$, and κ describe the effect of the remote bands on the $(\Gamma_8 + \Gamma_7)$ valence band of the semiconductor and can be expressed through the standard Luttinger constants γ_i^L and κ^L (see the Appendix). The parameter q , determining the cubic-in- \mathbf{J} valence-band spin splitting, is small and, hence, is dropped in the subsequent calculations. Following Foreman,¹⁹ we assume that the quadratic-in- \mathbf{k} conduction band term ($F + 1/2$) is zero in order to eliminate spurious solutions with very large real or imaginary wave vectors, as it was shown that this modification of the 8×8 Hamiltonian does not lead to a noticeable variation in the electron or hole dispersion. At the same time, it allows us to conveniently express the conduction-band envelope via wave function components in the valence band. For consistency we neglect the remote-band contributions to the g factor of conduction electrons; thus, g^0 in our calculation is equal to the Landé factor of free electrons ($\cong 2$). Again, as far as we focus on the states in the valence band, this can be done safely. The matrix elements of the bulk 8×8 Hamiltonian are given in the Appendix of Ref. 18.

The question of boundary conditions for multicomponent envelopes emerges as the top priority in heterostructures with abrupt interfaces. Imposing the continuity condition on the envelope functions $\varphi_n(z)$ as the first boundary condition and integrating the multiband Schrödinger equation over the interface region, we arrive at the second boundary condition which is defined by the particular relative order of the differentiation operators $k_z = -i\partial/\partial z$ and coordinate- (material-) dependent band structure parameters in the Hamiltonian. As this is not an issue in the bulk, the correct order of operators can be easily obscured or not even established firsthand. When one wishes to make a transition from the known bulk

TABLE I. “Bulk” hole g factors.

	Growth axis	In-plane
HH	$-6\kappa^L(0)$	0
LH	$-2\kappa^L(0)$	$-4\kappa^L(0)$
SO	$-4\kappa^L(-\Delta) - 2$	$-4\kappa^L(-\Delta) - 2$

to a heterostructure effective Hamiltonian, it becomes impossible to reestablish this order, which prevents one from establishing correct boundary conditions. The only easily understandable requirement to be fulfilled is that the Hamiltonian eigenenergies be real. This condition can be met, for example, by the frequently used procedure of the so-called Hamiltonian symmetrization that forces real eigenvalues (symbolically it can be presented as a substitution $Ak_\alpha k_\beta \rightarrow [k_\alpha A k_\beta + k_\beta A k_\alpha]/2$).

On the other hand, straightforward methods to construct a $\mathbf{k}p$ Hamiltonian for a heterostructure determine unambiguously the order of the operators and, hence, the set of the boundary conditions.^{20,21} Relocating all material-dependent parameters in the Ram-Mohan Hamiltonian¹⁸ in between the differentiation operators k_α, k_β (which is implicitly assumed anyway in all approaches) while keeping the operator order intact, we end up with the form of Hamiltonian with a correct order of operators that is exactly equivalent to one, consistently derived in Ref. 21. Note that Ram-Mohan *et al.*¹⁸ in their analysis used the symmetrization procedure instead. Still, as in any approach that explicitly accounts for the coupling with the conduction band, the questionable order of operators in Ref. 18 concerns only the remote-band terms. Thus, the significance of the problem is greatly reduced in comparison to, for example, more simple 6×6 valence band models that treat the conduction band as one of the remote bands. It turns out that in our particular case of LH states at the bottom of the subband (so as with $k_x = k_y = 0$), the result for the in-plane g factor is *completely* independent whether the symmetrization is applied or not.

IV. IN-PLANE COMPONENT OF THE LH g FACTOR

Let us start with a qualitative analysis of the limiting cases of very wide and very narrow QW's. Some simple conclusions can be made based solely on the form of the Hamiltonian itself, without any numerical calculations involved. For very wide QW's, we approach the case of a bulk semiconductor where the applied magnetic field freely mixes together LH and HH states forming a double ladder of Landau levels. When the magnetic field is still small in comparison to the quantization energies (or strain-induced splittings in the case of strained semiconductors), the explicit form of the 8×8 $\mathbf{k}p$ Hamiltonian allows one to obtain immediately the g factor components for all three hole subbands as summarized in Table I. The same is true in the case of ultranarrow QW's, where the parameters of the barrier layer define hole g factor tensors.

One immediately notes that the HH in-plane g factor is zero in this model (where, as we already mentioned, the small valence-band parameter q is neglected). Even with the

parameter q accounted for, the in-plane g factor value is too small for direct spectroscopic resolution of the HH sublevels in the available magnetic fields. The SO states cannot be made the ground hole state in typical III-V heterosystems. Ultimately, only the LH states show promise. Thus, one needs to design a structure where the LH subband will be pushed up by the intrinsic strain and evaluate the LH g factor where the renormalization of the bulk value is due to strain and quantum confinement in the QW structure. To achieve this goal, we apply the general recipe outlined in Sec. II.

The LH wave function $|\uparrow\rangle$ in QW's at the bottom of the subband ($k_x=k_y=0$) can be presented in the form

$$|\uparrow\rangle = u(z)|S\uparrow\rangle + v(z)|LH\uparrow\rangle + w(z)|SO\uparrow\rangle, \quad (3)$$

where u, v , and w are conduction band, LH, and SO z -dependent envelopes, respectively; Bloch amplitudes $|j\rangle$ for the 8×8 model are given in the Appendix. The set of functions $(u, v, -w)$ defines $|\downarrow\rangle$; it is a result of the particular choice of the phases in the Bloch amplitudes. HH states do not mix into functions $|\uparrow\rangle, |\downarrow\rangle$ at the bottom of the subband, simplifying derivations considerably. The electron envelope u can be expressed via the first-order derivatives of functions v and w as

$$(E_g - E)u = \sqrt{\frac{2}{3}}Pk_z v - \frac{1}{\sqrt{3}}Pk_z w. \quad (4)$$

Excluding $u(z)$, one finds that the functions $v(z)$ and $w(z)$ are solutions of a pair of second-order differential equations

$$\begin{pmatrix} -k_z \left[\frac{1}{2}g_1^L(E) + g_2^L(E) \right] k_z - E & \sqrt{2}k_z g_2^L(E)k_z \\ \sqrt{2}k_z g_2^L(E)k_z & -\frac{1}{2}k_z g_1^L(E)k_z - \Delta - E \end{pmatrix} \times \begin{pmatrix} v \\ w \end{pmatrix} = 0. \quad (5)$$

These equations are complimented by the boundary conditions at the heterostructure interfaces, requiring continuity of the envelopes (v, w) and combinations of their first derivatives $\partial H / \partial k_z(v, w)$, which together conserve electron flux through the interface. The valence-band offset V at the heterointerface should be incorporated into Eq. (5) when considering barrier layers in an obvious way through the substitution $E \rightarrow E + V$. The normalization condition must be applied to the total multicomponent wave function given by Eq. (3).

Our general procedure gives for the in-plane component of the LH g factor

$$g_{LH,\perp} = g_{\text{imp}} + g_{\text{exp}}, \quad (6)$$

where g_{imp} is a result of the evaluation of the first, vector-potential-related term in Eq. (2),

$$g_{\text{imp}} = 4 \int dz z \left[\frac{3}{\sqrt{2}} \gamma_3 (w^* v' - v^* w') + \frac{E_p}{3(E_g - E)} \times \left(v^* v' - \frac{1}{\sqrt{2}} v^* w' + \sqrt{2} w^* v' - w^* w' \right) \right], \quad (7)$$

while g_{exp} comes from the second term responsible for direct interaction with the magnetic field,

$$g_{\text{exp}} = 4 \int dz \left[\frac{1}{2} |u|^2 - \kappa |v|^2 + \left(\kappa + \frac{1}{2} \right) |w|^2 - \frac{1}{\sqrt{2}} (\kappa + 1) \times (v^* w + w^* v) \right]. \quad (8)$$

In the last equation we decided not to express the envelope u via functions v and w utilizing Eq. (4), as the present form produces a more transparent result with terms that simply account for the direct interaction with the magnetic field in the bulk conduction, LH, and SO bands. For the localized LH states v and w are real and u is pure imaginary.

The theory developed thus far is equally applicable to any cubic semiconductor with a band structure similar to that shown in Fig. 1. This includes both III-V and II-VI pure compounds and solid solutions. With the strain-induced energy shifts included, wurtzite crystals can be analyzed as well in the framework of the quasicubic model that treats wurtzite crystal as a strained cubic one.

In our analysis, we assume the structure to be grown pseudomorphically on an unstrained substrate. The choice of the substrate composition will define the common in-plane lattice constant a_{sub} and, consequently, strains in the heterostructure layers: $\varepsilon_{\perp} \equiv \varepsilon_{xx} = \varepsilon_{yy} = a_{\text{sub}}/a_0 - 1$, $\varepsilon_{\parallel} \equiv \varepsilon_{zz} = -2C_{12}/C_{11}\varepsilon_{\perp}$. The C_{ij} are the bulk elastic moduli. Shifts of the conduction- and valence-band edges due to the strain are defined by the deformation potentials and should be incorporated into the calculation procedure via the 8×8 \mathbf{kp} effective Hamiltonian. In the first-order approximation, the energy displacement of the Γ_6 minimum is linear in strain. By symmetry, this shift can be written as

$$\delta E_c = e_c \varepsilon, \quad (9)$$

where we used notation $\varepsilon = \varepsilon_{xx} + \varepsilon_{yy} + \varepsilon_{zz}$.

For the relevant strain-induced shifts in the valence band, we have

$$\begin{aligned} \delta E_{\text{HH}} &= a_v \varepsilon - b_v (\varepsilon_{\parallel} - \varepsilon_{\perp}), \\ \delta E_{\text{LH}} &= a_v \varepsilon + b_v (\varepsilon_{\parallel} - \varepsilon_{\perp}), \end{aligned} \quad (10)$$

$$\delta E_{\text{SO}} = a_v \varepsilon,$$

$$\delta E_{\text{LH,SO}} = -\sqrt{2} b_v (\varepsilon_{\parallel} - \varepsilon_{\perp}),$$

where a_v, b_v are the valence-band deformation potentials in the standard Bir-Pikus notation.²² All shifts are diagonal with respect to the spin-up, spin-down electron and hole states.

TABLE II. Parameters of the band structure for III-V semiconductors.

	GaAs	GaP	InAs	InP
E_g (eV)	1.519	2.895	0.418	1.424
Δ (eV)	0.341	0.080	0.38	0.108
E_p (eV)	28.9	~ 25	22.1	20.4
$\gamma_1^L(0)$	6.85	4.2	19.7	5.0
$\gamma_2^L(0)$	2.10	0.98	8.4	1.6
$\gamma_3^L(0)$	2.90	1.66	9.3	2.0
$\kappa^L(0)$	1.2	0.34	7.68	0.97
a_0 (Å)	5.652	5.447	6.048	5.859
C_{11} (10^{11} dyn cm $^{-2}$)	11.26	14.05	8.33	10.11
C_{12} (10^{11} dyn cm $^{-2}$)	5.71	6.2	4.53	5.61

V. NUMERICAL EXAMPLE AND DISCUSSION

For numerical illustration we have chosen structures with both well and barrier materials based on the quaternary solid solution $\text{In}_{1-x}\text{Ga}_x\text{As}_y\text{P}_{1-y}$, which is useful for 1.3 and 1.55 μm optoelectronic applications. Although as its particular representative we use here only the most widely utilized $\text{In}_{1-x}\text{Ga}_x\text{As}/\text{InP}$ heterosystem, we decided to prepare our numerical procedure and data, so that they are readily applicable to more general, two-parameter material compositions for each heterolayer. Band structure parameters for constituent pure compounds are given in Table II. Complete knowledge of the detailed band structure is unavailable at present for all InGaAsP solid solutions. Thus, based on the values in Table II, we use an interpolation scheme for solutions with different (x,y) compositions. For the band gap we apply an equation given in Ref. 23 (with a proper adjustment for the low-temperature regime):

$$E_g = 1.424 + 0.713x - 1.084y + 0.758x^2 + 0.078y^2 - 0.078xy - 0.322x^2y + 0.03xy^2 \quad (\text{in eV}). \quad (11)$$

For other parameters of the band structure (Δ, E_p , modified — only remote band contributions — Luttinger parameters γ_i, κ) we apply a bilinear interpolation of values for pure semiconductors. Slightly different interpolation schemes were also proposed;²⁴ in common, they have an important provision that, while interpolating, conduction band contribution to conventional Luttinger parameters should be treated separately and diversely from remote-band contributions.

The lattice mismatch between solid solutions with different compositions in the InGaAsP family can reach 8%. The absence of reliable deformation potentials for InGaAsP solid solutions and drastic scattering of data for the respective pure III-V semiconductors suggests choosing some average values for all compositions and not applying an interpolation scheme. For our calculation we use $e_c = 10$ eV, $a_v = -0.7$ eV, and $b_v = -1.7$ eV.

An interesting question arises concerning the values of the conduction- and valence-band offsets at the heterointerfaces in the InGaAsP family. The only systematic measurements found are for the lattice-matching $\text{In}_{0.53+0.47y}\text{Ga}_{0.47y}\text{As}_y\text{P}_{1-y}$

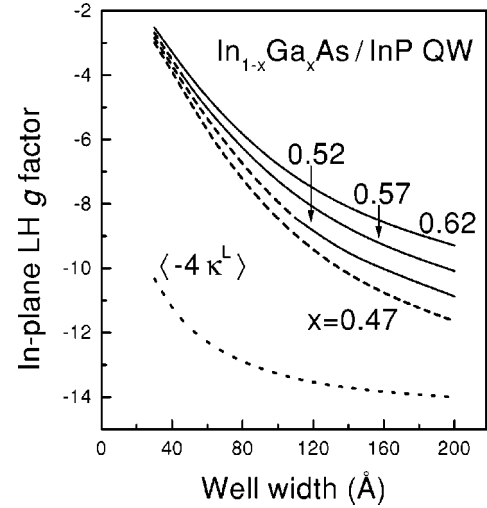


FIG. 2. The in-plane LH g factor in $\text{In}_{1-x}\text{Ga}_x\text{As}/\text{InP}$ QW as a function of the well layer width. Solid and dashed lines present results of the calculation using Eq. (6). Depending on the QW width and intrinsic strain defined by the InGaAs layer composition x , either the HH or LH subband acts as a ground hole state in the QW; this information is delivered by the line type: dashed and solid lines, respectively. The dotted line visualizes the naive approach based on the averaging of the material-dependent Luttinger parameter $\kappa^L(E)$ (“bulk” in-plane LH g factor) with probabilities to find the hole in the well and barrier layers.

solid solutions grown on an InP substrate, where the conduction-band offset is $\Delta E_c = 288y + 3y^2$ meV.²⁵ In view of the lack of other reliable information, we therefore assume that this dependence governs the offsets ratio $\Delta E_c/\Delta E_v$ on the (x,y) compositions plane along the line $(0.47y,y)$ of lattice matching quaternary compounds, and for points off the line we take the nearest point on the line to define $\Delta E_c/\Delta E_v$.

Figure 2 presents calculated g factor values for a free (not bound in the exciton or localized) LH in the unstrained as well as strained InGaAs/InP heterostructures as a function of the InGaAs layer thickness. We repeat that the orientation of the applied magnetic field was assumed to be in-plane. The calculation was carried out for the hole states at the bottom of the LH subband in the single QW structure. Both solid and dashed curves are produced using the procedure outlined above; a solid line is used when the LH forms the ground hole state while the dashed line is used otherwise. Depending on the concurrent effects of the strain caused by the lattice constant mismatch and the quantum confinement, either LH’s or HH’s form the ground hole states. In very wide wells, strain alone defines the order of levels. If the effects of strain and confinement are opposite in sign, a crossover in the character of the ground state happens at some intermediate well width, below which the effect of confinement prevails. We emphasize again that we are primarily interested in the structure with the ground hole state formed by the LH. Our calculation gives dependences that are steep at small layer thicknesses, but asymptotically approach their respective “bulk” values for very wide QW’s. Though not explicitly present in Fig. 2, at very narrow well widths (where the

applicability of the macroscopic kp method itself can probably be questioned) the in-plane LH g factor crosses zero for our heteropair choice. In this case, there will be no Zeeman splitting of the spin-up and spin-down LH states. For the purposes of the quantum receiver,⁵ one should avoid this region of well widths. Indeed, the g factor should be kept at a reasonably large value, which we have shown is feasible for a broad range of structure widths.

Results of the unsophisticated approach, meaning simple averaging of the (energy-dependent) “bulk” in-plane values for LH’s (given in Table I) with quantum-mechanical probabilities to find particle in different heterolayers, are also given in Fig. 2 as the dotted line. By no means simple averaging can be considered as a satisfactory procedure.

VI. SUMMARY

We have studied the effect of an external in-plane magnetic field on the structure of LH states in semiconductor heterostructures with a single QW. The hole states were found in the framework of the sophisticated 8×8 kp model. The dependences of the in-plane LH g factor on the QW parameters for both lattice-matched and -strained InGaAs/InP heterosystems were calculated. Significantly, the in-plane LH g factors in heterostructures differ radically from the value $-4\kappa^L$, which should be considered to be the effective transverse LH g factor for a bulk semiconductor. Only in the limiting cases does the g factor in QW approach this value.

ACKNOWLEDGMENTS

This work has been supported, in part, by the Defense Advanced Research Projects Agency and the Office of Naval Research. A.A.K. would like to thank D. Kahn for a critical reading of the manuscript.

APPENDIX

The Bloch amplitudes $|j\rangle$, which are eigenstates of the conduction and valence bands at the Γ point, can be ex-

pressed through Kane basis functions S , X , Y , and Z in the following way:

$$\begin{aligned} |1\rangle &= |S\uparrow\rangle, \\ |2\rangle &= |\text{HH}\uparrow\rangle = -i/\sqrt{2}|(X+iY)\uparrow\rangle, \\ |3\rangle &= |\text{LH}\downarrow\rangle = i/\sqrt{6}|(X-iY)\uparrow + 2Z\downarrow\rangle, \\ |4\rangle &= |\text{SO}\downarrow\rangle = -i/\sqrt{3}|(X-iY)\uparrow - Z\downarrow\rangle, \\ |5\rangle &= |S\downarrow\rangle, \\ |6\rangle &= |\text{LH}\uparrow\rangle = -i/\sqrt{6}|(X+iY)\downarrow - 2Z\uparrow\rangle, \\ |7\rangle &= |\text{HH}\downarrow\rangle = i/\sqrt{2}|(X-iY)\downarrow\rangle, \\ |8\rangle &= |\text{SO}\uparrow\rangle = -i/\sqrt{3}|(X+iY)\downarrow + Z\uparrow\rangle. \end{aligned} \quad (\text{A1})$$

The modified Luttinger parameters γ_i and κ determine the influence of the remote bands on the valence band of a semiconductor ($\Gamma_7 + \Gamma_8$) and define the energy-dependent Luttinger parameters γ_i^L and κ^L as

$$\begin{aligned} \gamma_1^L(E) &= \gamma_1 + E_p/3(E_g - E), \\ \gamma_2^L(E) &= \gamma_2 + E_p/6(E_g - E), \\ \gamma_3^L(E) &= \gamma_3 + E_p/6(E_g - E), \\ \kappa^L(E) &= \kappa + E_p/6(E_g - E). \end{aligned} \quad (\text{A2})$$

Values of $\gamma_i^L(0), \kappa^L(0)$ are typically presented in the literature as they are derived from measurements on the hole states at the top of the valence band in bulk semiconductors. They are simply denoted then as γ_i^L, κ^L . In the presence of strain, an additional term (i.e., strain-induced shift of the conduction band δE_c) should be incorporated into the energy denominators. The shift in the valence band will be accounted for by the changes in the energy of the LH state E .

*Electronic address: kiselev@eos.ncsu.edu

¹A. Zeilinger, Phys. World, Special Issue (March 1998), p. 35; W. Tittel, G. Ribordy, and N. Gisin, *ibid.*, p. 41.

²J. I. Cirac, P. Zoller, H. J. Kimble, and H. Mabuchi, Phys. Rev. Lett. **78**, 3221 (1997).

³T. Pellizari, Phys. Rev. Lett. **79**, 5242 (1997).

⁴G. E. Pikus and A. N. Titkov, in *Optical Orientation*, edited by F. Meier and B. P. Zakharchenya (Elsevier, New York, 1994), p. 73.

⁵R. Vrijen and E. Yablonovitch, quant-ph/0004078 (unpublished).

⁶L. M. Roth, B. Lax, and S. Zwerdling, Phys. Rev. **114**, 90 (1959).

⁷E. L. Ivchenko and A. A. Kiselev, Sov. Phys. Semicond. **26**, 827 (1992).

⁸A. A. Kiselev, E. L. Ivchenko, and U. Rössler, Phys. Rev. B **58**, 16 353 (1998).

⁹See, for example, M. J. Snelling, G. P. Flinn, A. S. Plaut, R. T. Harley, A. C. Tropper, R. Eccleston, and C. C. Phillips, Phys.

Rev. B **44**, 11 345 (1991); V. K. Kalevich and V. L. Korenev, JETP Lett. **56**, 257 (1992); B. Kowalski, P. Omling, B. K. Meyer, D. M. Hofmann, C. Wetzel, V. Härle, F. Scholz, and P. Sobkowicz, Phys. Rev. B **49**, 14 786 (1994); R. M. Hannak, M. Oestreich, A. P. Heberle, W. W. Rühle, and K. Köhler, Solid State Commun. **93**, 313 (1995); A. A. Sirenko, T. Ruf, K. Eberl, M. Cardona, A. A. Kiselev, E. L. Ivchenko, and K. Ploog, in *High Magnetic Fields in Semiconductor Physics*, edited by G. Landwehr and W. Ossau (World Scientific, Singapore, 1996), p. 561; Q. X. Zhao, M. Oestreich, and N. Magnea, Appl. Phys. Lett. **69**, 3704 (1996); P. Le Jeune, D. Robart, X. Marie, T. Amand, M. Brousseau, J. Barrau, V. Kalevich, and D. Rodichev, Semicond. Sci. Technol. **12**, 380 (1997); A. A. Sirenko, T. Ruf, M. Cardona, D. R. Yakovlev, W. Ossau, A. Waag, and G. Landwehr, Phys. Rev. B **56**, 2114 (1997); A. Malinowski and R. T. Harley, *ibid.* **62**, 2051 (2000).

¹⁰A. A. Kiselev and L. V. Moiseev, Phys. Solid State **38**, 866 (1996).

- ¹¹A. A. Kiselev, E. L. Ivchenko, A. A. Sirenko, T. Ruf, M. Cardona, D. R. Yakovlev, W. Ossau, A. Waag, and G. Landwehr, *J. Cryst. Growth* **184/185**, 831 (1998).
- ¹²X. Marie, T. Amand, P. Le Jeune, M. Paillard, P. Renucci, L. E. Golub, V. D. Dymnikov, and E. L. Ivchenko, *Phys. Rev. B* **60**, 5811 (1999).
- ¹³J. M. Luttinger and W. Kohn, *Phys. Rev.* **97**, 869 (1955).
- ¹⁴J. M. Luttinger, *Phys. Rev.* **102**, 1030 (1956).
- ¹⁵R. Eppenga, M. F. H. Schuurmans, and S. Colak, *Phys. Rev. B* **36**, 1554 (1987).
- ¹⁶E. O. Kane, *J. Phys. Chem. Solids* **1**, 249 (1957).
- ¹⁷M. H. Weiler, in *Semiconductors and Semimetals*, edited by R. K. Willardson and A. C. Beer (Academic, New York, 1981), Vol. 16, p. 119.
- ¹⁸L. R. Ram-Mohan, K. H. Yoo, and R. L. Aggarwal, *Phys. Rev. B* **38**, 6151 (1988).
- ¹⁹B. Foreman, *Phys. Rev. B* **56**, 12 748 (1997).
- ²⁰M. G. Burt, *J. Phys.: Condens. Matter* **4**, 6651 (1992).
- ²¹B. Foreman, *Phys. Rev. B* **48**, 4964 (1993).
- ²²G. L. Bir and G. E. Pikus, *Symmetry and Strain-Induced Effects in Semiconductors* (Wiley, New York, 1974).
- ²³*Intrinsic Properties of Group IV Elements and III- V, II-VI, and I-VII Compounds*, edited by O. Madelung, Landolt-Börnstein, New Series, Group III, Vol. 22, Pt. A (Springer, Berlin, 1987); *Semiconductors — Basic Data*, edited by O. Madelung (Springer, Berlin, 1996).
- ²⁴C. M. de Sterke, *Phys. Rev. B* **36**, 6574 (1987).
- ²⁵S. Adachi, *Physical Properties of III-V Semiconductor Compounds: InP, InAs, GaAs, GaP, InGaAs, and InGaAsP* (Wiley, New York, 1992).